PB87-179271

Parameter Monitoring for Real-Time Electrostatic Precipitator Troubleshooting

(U.S.) Environmental Protection Agency
Research Triangle Park, NC

Apr 87

U.S. Department of Commerce
National Technical Information Service
NTIS

PB87-179271

EPA/600/D-87/070
April 1987

PARAMETER MONITORING FOR REAL-TIME ELECTROSTATIC PRECIPITATOR TROUBLESHOOTING

by

Phil A. Lawless and David S. Ensor
Research Triangle Institute
Research Triangle Park, NC 27711

Leslie E. Sparks
Air and Energy Engineering Research Laboratory
U.S. Environmental Protection Agency
Research Triangle Park, NC 27711

CR810152

EPA Project Officer
Dale L. Harmon

AIR AND ENERGY ENGINEERING RESEARCH LABORATORY
OFFICE OF RESEARCH AND DEVELOPMENT
U.S. ENVIRONMENTAL PROTECTION AGENCY
RESEARCH TRIANGLE PARK, NC 27711

REPRODUCED BY
U.S. DEPARTMENT OF COMMERCE
NATIONAL TECHNICAL
INFORMATION SERVICE
SPRINGFIELD, VA. 22161

TECHNICAL REPORT DATA
(Please read Instructions on the reverse before completing)

1. REPORT NO.	2.	3. RECIPIENT'S ACCESSION NO.
EPA/600/D-87/070		

4. TITLE AND SUBTITLE	5. REPORT DATE
Parameter Monitoring for Real-Time Electrostatic Precipitator Troubleshooting	April 1987
	6. PERFORMING ORGANIZATION CODE
7. AUTHOR(S)	8. PERFORMING ORGANIZATION REPORT NO.
P. A. Lawless and D. S. Ensor (RTI), and L. E. Sparks (EPA)	
9. PERFORMING ORGANIZATION NAME AND ADDRESS	10. PROGRAM ELEMENT NO.
Research Triangle Institute P. O. Box 12194 Research Triangle Park, North Carolina 27709	11. CONTRACT/GRANT NO. CR810152
12. SPONSORING AGENCY NAME AND ADDRESS	13. TYPE OF REPORT AND PERIOD COVERED
EPA, Office of Research and Development Air and Energy Engineering Research Laboratory Research Triangle Park, NC 27711	Published Paper; 3-8/85 14. SPONSORING AGENCY CODE EPA/600/13

15. SUPPLEMENTARY NOTES AEERL project officer is Dale L. Harmon, Mail Drop 61, 919/541-2429.

16. ABSTRACT The paper discusses detailed numerical calculations of particle charge and extinction coefficient performed using current models. (NOTE: Both the electrical saturation charge and the optical cross section of particles exiting an electrostatic precipitator are roughly proportional to the square of the particle diameter, suggesting a significant relationship between them.) The results suggest that information about rapping reentrainment, back corona, and, possibly, sulfuric acid condensation can be gained from simultaneous outlet measurements of opacity and space charge. Some experimental observations based on semicontinuous measurements have confirmed these results in a general way and point to the use of the method as a precipitator diagnostic tool.

17. KEY WORDS AND DOCUMENT ANALYSIS

a. DESCRIPTORS		b. IDENTIFIERS/OPEN ENDED TERMS	c. COSATI Field/Group	
Pollution	Space Charge	Pollution Control	13B	20C
Electrostatic Precipitators	Absorptivity	Stationary Sources		
	Opacity	Troubleshooting	13I	
Maintenance	Measurement	Back Corona	15E	14B
Mathematical Models			12A	
Particles	Electric Corona		14G	

18. DISTRIBUTION STATEMENT	19. SECURITY CLASS (This Report)	21. NO. OF PAGES
Release to Public	Unclassified	16
	20. SECURITY CLASS (This page)	22. PRICE
	Unclassified	

EPA Form 2220-1 (9-73)

PARAMETER MONITORING FOR REAL-TIME ELECTROSTATIC PRECIPITATOR TROUBLESHOOTING

Phil A. Lawless and David S. Ensor
Research Triangle Institute
P.O. Box 12194
Research Triangle Park, North Carolina 27709

Leslie E. Sparks
Air and Energy Engineering Research Laboratory
U.S. Environmental Protection Agency
Research Triangle Park, North Carolina 27711

Abstract

Both the electrical saturation charge and the optical cross section of particles exiting an electrostatic precipitator (ESP) are roughly proportional to the square of the particle diameter, suggesting a significant relationship between them. Detailed numerical calculations of particle charge and extinction coefficient have been performed using current models. The results suggest that information about rapping reentrainment, back corona, and, possibly, sulfuric acid condensation can be gained from simultaneous outlet measurements of opacity and space charge. Some experimental observations based on semicontinuous measurements have confirmed these results in a general way and point to the use of the method as a precipitator diagnostic tool.

Introduction

Electrostatic precipitators (ESPs) are widely applied for the control of particulate emissions from boilers, kilns, smelters, and furnaces. In the course of operation, the emissions from the ESP are usually monitored by a transmissometer (opacity meter), which provides information about the performance of the unit. For instance, rapping emissions appear as spikes in opacity over a continuous background. It should be possible, by measuring the state of charge on the particles leaving the ESP, to determine how well the unit is performing electrically in its goal of charging and collecting particles.

In a recent precipitator emissions test, particulate space charge was measured to provide data to test an ESP performance model. The results of the test and the model predictions have contributed to an appreciation of the potential for this type of monitoring.

Theoretical Background

To understand how particle charge and opacity might be related, simplified theories for each will be considered. These are limiting cases, applicable to "large" particles only, but the results are qualitatively correct.

Particle Charging

For particles larger than 3-5 μm in diameter, the charge quickly reaches a limiting value, the field saturation charge.[1] For conductive particles or low resistivity particles, this charge, q_s, is given by:

$$q_s = 12\pi\varepsilon_o E r^2, \tag{1}$$

where ε_o is the free-space permittivity; E, the electric field in which the particle was charged; and r, the particle radius. The appropriate field to use is the highest field strength to which the particles were exposed, because once charged, the particles do not lose any charge.

Opacity and Extinction Coefficient

Opacity is a quantity related to the transmissivity of light over a definite path length:

$$\text{Opacity } (\%) = 100(1-T), \tag{2}$$

where T is the transmissivity of the medium. The transmissivity is the measured quantity and is given by:

$$T = I/I_o, \tag{3}$$

where I is the intensity of light measured through the obscuring medium, and I_o is the intensity of light through a perfectly transparent medium of the same path length.

Assuming the Beer-Lambert Law of scattering, an extinction coefficient, b_{ext}, can be defined by:

$$b_{ext} = -\ln(I/I_o)/L, \tag{4}$$

where L is the path length over which the light intensities are measured. The total extinction coefficient is made up of the contributions from each particle size times the number density of particles of that size:

$$b_{ext} = \sum_i b_{ext}(i)N(i), \tag{5}$$

where i indicates a particle size, $b_{ext}(i)$ is the extinction coefficient for that size, and N(i) is the number of particles per unit volume for that size.

The extinction coefficient for a given particle radius, r, is given by:

$$b_{ext}(r) = Q_{ext}(x)\pi r^2, \tag{6}$$

where $Q_{ext}(x)$ is the scattering coefficient, and x is a dimensionless parameter relating the particle diameter to the wavelength of light, λ, used:

$$x = 2\pi r/\lambda. \tag{7}$$

From Mie scattering theory, Q_{ext} can be evaluated exactly, given the index of refraction of the particles. For the purposes of this work, it suffices to note that for $x > 10$ and weakly absorbing particles, such as flyash, the extinction coefficient for large particles is given, approximately, by:

$$b_{ext}(r) = 2\pi r^2. \tag{8}$$

Theoretical Results for Small Particles

Generally, the charge that can be acquired on small particles rises above the saturation value given by Equation 1 because of the influence of thermal excitation of ions over the repulsive barrier created by the charge already on the particle. On the other hand, the extinction coefficient for very small particles approaches the Rayleigh scattering limit, in which the scattering coefficient varies as r^4, for overall variation of r^6. Thus the behavior of particle charge and extinction coefficient differs radically in the small particle range.

Average Properties for Large Particle Ensembles

In practical terms, the measurable quantities of interest are the optical transmissivity and the total particulate space charge. If we confine the region of interest to large particles only, we can obtain the following relations:

$$Q = \sum_r q_s(r)N(r), \tag{9}$$

where Q is the particulate space charge, $q_s(r)$ is the saturation charge from Equation 1, and N(r) is the number density of particles of size r; and,

$$b_{ext} = \sum_r b_{ext}(r)N(r), \tag{10}$$

where $b_{ext}(r)$ is the extinction coefficient given by Equation 8.

Forming the ratio, which we call "Q/b," we obtain

$$Q/b = \frac{\sum_r 12\pi\varepsilon_o E r^2 N(r)}{\sum_r 2\pi r^2 N(r)}, \tag{11}$$

which reduces to:

$$Q/b = 6\varepsilon_o E. \tag{12}$$

This simple result shows that the ratio Q/b expressly measures the electrical conditions experienced within the precipitator.

ESP Model and Detailed Calculations

The ESP performance model which was used for performing detailed calculations of Q/b has been described.[2] This model incorporates a continuum particle-charging module capable of evaluating the charge on

small, intermediate, and large particles. It incorporates calculations of the electric field corresponding to measured voltage and current operating points. It has a module for calculating the opacity of the particulate emissions, corresponding to the Mie scattering amplitudes for small, intermediate, and large particles.

The calculations in the model are carried out independently for discrete particle sizes in the range of 0.1-50 μm. The total particulate space charge and extinction coefficient are calculated, and the relative contribution of each particle size is available too. Referring to Equations 9 and 10, it can be seen that the size distribution plays a significant role in determining the relative contributions of each size to the whole.

The calculations were carried out for five precipitators considered free from back corona and for one on which measurements of space charge and opacity were performed. The relative fractions for four different units are shown in Figure 1. In all four units shown in Figure 1, it should be noted that the space charge and extinction coefficients vary almost identically for particles above 3 μm. This is a good indication that Equation 12 applies in this region.

The first ESP, Unit 1, had a large fraction of its particles below 0.5 μm. This led to a highly charged submicron fraction which did not contribute significantly to the optical extinction coefficient. Despite the large number of submicron particles, most of the mass was carried in particles greater than 3 μm.

Unit 2 was a hot-side ESP. The number of particles below 0.5 μm dropped rapidly, but there was a pronounced peak in the mass distribution (and number distribution, too) at 3 μm. This corresponds to a region where $Q_{ext}(x)$ can vary rapidly as a function of x; it is borne out in the variation of the extinction coefficient.

In Unit 3, a cold-side unit, there was a fair amount of mass below 1 μm, but not much below 0.3 μm. The extinction coefficient peaked sharply at 0.7 μm because of the variation of $Q_{ext}(x)$, but the peak in the particulate charge was less pronounced. The particles below 0.5 μm carry a significant fraction of the total charge but do not influence the extinction coefficient very much.

In Unit 4 there were almost no particles below 0.5 μm, and the space charge follows the extinction coefficient over most of the range.

A summary of the calculations of total Q/b is presented in Table I. It can been seen that Q/b for all particle sizes is always greater than that for particles larger than 3 μm in diameter. The calculations of $6\varepsilon_o E_o$ were made using the precipitator model to provide the maximum average field the particles experienced. The values agree fairly well with Q/b for particles larger than 3 μm.

Experimental Measurements

During a field test at Precipitator 1, simultaneous measurements of particle space charge and opacity were made. The opacity was measured with the plant's stack transmissometer and the space charge with a Faraday cage filter method.[3]

The opacity spikes during rapping were not well resolved in time on the transmissometer chart, but independent real-time measurements gave a

determination of their width. A composite opacity, consisting of a time-weighted average of the spikes and the baseline, was calculated.

The particulate charge was measured with an electrometer connected to a Faraday cage sampling particulate inside the stack. The charge was accumulated for about 2 hours, and the volume of gas sampled was measured with a gas-sampling train and dry-gas meter.

Results

The space charge was measured on three separate days and was remarkably constant. The opacity varied considerably as a function of boiler demand, but most of the variation was caused by the rapping emissions. During the first two space charge measurements, it was observed that occasional rapping emissions would appear as steps in the accumulated charge. The effect was noticeable enough that the third measurement was correlated with the rapper program to identify the sections causing the steps.

In Table II, the results of the three runs are shown, with the third run broken into a total measurement and a non-rapping measurement. This division was made for three reasons: the rapping contributions were much greater than on the previous runs; the rapper program showed that inlet field raps were obvious at the outlet; and the charge contribution from the rapping emissions was of the opposite sign from the non-rapping emissions.

The difference in sign shows up in Table II as a reduced total charge and a drastically reduced Q/b from the more normal operation. If an instantaneous measurement for the space charge were used, then Q/b would have been negative during the rapping spikes and the difference would have been even more outstanding.

The model calculations for Q/b (Unit 1 from Table I) are in reasonable agreement with the measurements if we consider only particles larger than 3 μm in diameter. However, the model predicts that the Q/b for all particles should be almost twice the value measured. The failure of the precipitator to achieve this value is suspected to be due to back corona.

Back corona was likely in this precipitator because of the resistivity of the flyash, the high corona current densities, and the voltage current characteristics. It was not directly confirmed because the ash had a carbon content of 20-25 percent and because the corona was positive, which gives a less characteristic indication of back corona than does negative corona.

Interpretation of Measurements

Without further validation of the theoretical calculations with experimental measurements, it is risky to predict the full extent to which Q/b measurements can be put to use. Some generalizations can be stated despite lack of confirming evidence.

First, Equation 12 represents an idealized limit for Q/b for large particles. The nature of the charging process and opacity characteristics for fine particles dictate that this is a lower limit for a properly operating precipitator. The discrepancy between the calculated Q/b and measured values would be dependent on the particle size distribution, with the submicron fraction having a major influence on the ratio. In a practical sense, a measurement of Q/b at the outlet of an ESP would also be an average over all the charging zones. This could produce a Q/b lower than predicted by Equation 12.

When using Equation 12 to relate measured Q/b to the electrical conditions, sufficient accuracy in the electric field should be obtained by dividing the operating voltage by the wire to plate separation.

Second, as shown in the experimental measurements, Q/b can indicate a problem of excessive rapping emissions. This problem would appear in opacity measurements alone, but should be more sensitively indicated by the Q/b technique. If the rapping emissions do not cause Q/b to change, it would indicate that the reentrained particulate is being adequately recharged. The indications in the field test were that particles were not being recharged.

Third, back corona is generally considered to reduce particle charge and increase emissions. This would be evident in a value for Q/b that is less than theoretically predicted, either by the full-scale model or by Equation 12. Comparative measurements over a period of time would be a valuable diagnostic tool for this purpose. If a normal Q/b can be determined, then a drift to lower values could indicate the onset of back corona.

Several hypothetical treatments of these cases will be discussed in the following paragraphs. Assuming that continuous measures of space charge and opacity are available, the quotient Q/b can be obtained by digitizing the signals and performing the operations mathematically. Alternatively, the logarithm of the quotient can be displayed in analog fashion as the difference of the logarithms of Q and b.

First, consider rapping emissions. Particles collected on the plates will lose their acquired charge and, when rapped off, may be charged oppositely (by induction), be neutral, or have a fraction of the normal charge (due to surface charging). Subsequent ion charging will modify these charges, but sometimes so much material is involved that the charging is far from complete.

In Figure 2, a series of rapping spikes are shown where the rapped particles reacquire most of their normal charge. The intensity of the rapping emissions is shown increasing in time. Since the amount of charged material increases during the rapping spike, both the opacity (or b) and the space charge show increases. However, Q/b shows decreasing spikes since most rapped material is larger than 3 μm in diameter.

In Figure 3, a similar series occurs in which the rapped material remains uncharged, perhaps due to sneakage through the hoppers. In this case, opacity increases but the space charge shows no change. Q/b is more strongly affected than in the previous case.

In Figure 4, the rapped material retains a charge of the opposite polarity. Here, the space charge shows reductions during the spikes and Q/b is very strongly affected. This kind of situation would indicate serious rapping emissions because of the overloaded charging zones of the ESP.

Figure 5 shows what might happen if a section failure occurred. Both the opacity and space charge would increase dramatically, but the Q/b quotient would remain essentially unchanged because the electrical charging conditions are unmodified. The rapping spikes might be more affected by the reduction of potential recharging. This type of response would aid in the rapid diagnosis of such a failure.

Figure 6 shows a gradual onset of back corona, with an increasing opacity, decreasing space charge, and even more rapidly decreasing Q/b. Although this is not a perfect indication of back corona, in conjunction with other observations, it would be strongly indicative of the condition.

Continuous Monitoring

In order for this technique to be useful, it should be at least as easy to use as the opacity measurement itself.

A continuous method would be to measure the electric field in the duct, or stack, near the location for measuring opacity. Using Gauss' Law, the field at the surface would be related to the space charge by:

$$\int_S \vec{E} \cdot \vec{ds} = \int_V \frac{Q}{\varepsilon_o} \, dV, \tag{13}$$

where S is the surface enclosing the volume V and ε_o is the free-space permittivity. If we assume a long cylindrical duct of diameter R, symmetry allows the evaluation of the integrals:

$$E \cdot 2\pi R = (Q/\varepsilon_o) \, \pi R^2, \tag{14}$$

so that Q can be evaluated:

$$Q = 2\varepsilon_o E/R. \tag{15}$$

In other duct geometries, a similar expression could be obtained, differing primarily in the numerical constants. Thus, the problem of measuring Q in the stack can be replaced by an electric field measurement at the surface of the stack.

Alternatively, a large capacity Faraday cage could be used, with the space charge obtained from the current and gas volume flowing through the device. With size selective inlets, the large and small particle contributions to space charge could be separated.

Summary

It has been shown by a simple model that the ratio of space charge to extinction coefficient is directly related to the charging conditions in an ESP. Detailed model calculations have also indicated the relation, as well as showing that the simple model represents a lower bound in a properly operating precipitator.

It is proposed that monitoring Q/b will reveal problems in the precipitator that are associated with back corona, rapping emissions, and possibly fume formation. Measurements on a running precipitator have been made, and confirm that these judgments are at least qualitatively correct.

Making the space-charge measurement is potentially no more difficult than making the opacity measurement, and continuous operation of a Q/b monitor should be useful in precipitators whose performance is critical or experiencing problems.

References

1. H. W. White, Industrial Electrostatic Precipitation. Addison-Wesley, Reading, Mass., 1963.

2. P. A. Lawless, J. W. Dunn, and L. E. Sparks, "A Computer Model for ESP Performance." In: Third Symposium on the Transfer and Utilization of Particulate Control Technology, Volume II, EPA-600/9-82-005b, (NTIS PB83-149591), pp. 44-53 (1982).

3. M. Durham, G. Rinard, D. Rugg, and L. Sparks, "Measurement and Interpretation of Current Density Distribution and Charge/Mass Data." In: Third Symposium on the Transfer and Utilization of Particulate Control Technology, Volume II, EPA-600/9-82-005b (NTIS PB83-149591), pp. 54-65 (1982).

TABLE I. THEORETICAL RATIO OF SPACE CHARGE TO EXTINCTION COEFFICIENT

Unit	Q/b ($\mu C/m^2$) (all particles)	Partial Q/b ($\mu C/m^2$) ($\geq$ 3.0 μm)	$6\varepsilon_o E$ ($\mu C/m^2$)
1	23.4	9.1	8.0
2	21.6	17.2	15.4
3	19.9	15.1	17.5
4	24.4	22.4	20.2
5 (same unit as 2; different test data)	23.9	15.7	12.5
6	19.0	14.9	14.9

TABLE II. MEASURED SPACE CHARGE AND EXTINCTION COEFFICIENTS

Run	b_e (m^{-1})	Q (C/m^3)	Q/b ($\mu C/m^2$)
1	0.011	1.7×10^{-7}	15.6
2	0.019	1.7×10^{-7}	8.9
3 (nonrap)	0.012	1.3×10^{-7}	10.8
3 (total)	0.026	9.3×10^{-8}	3.6

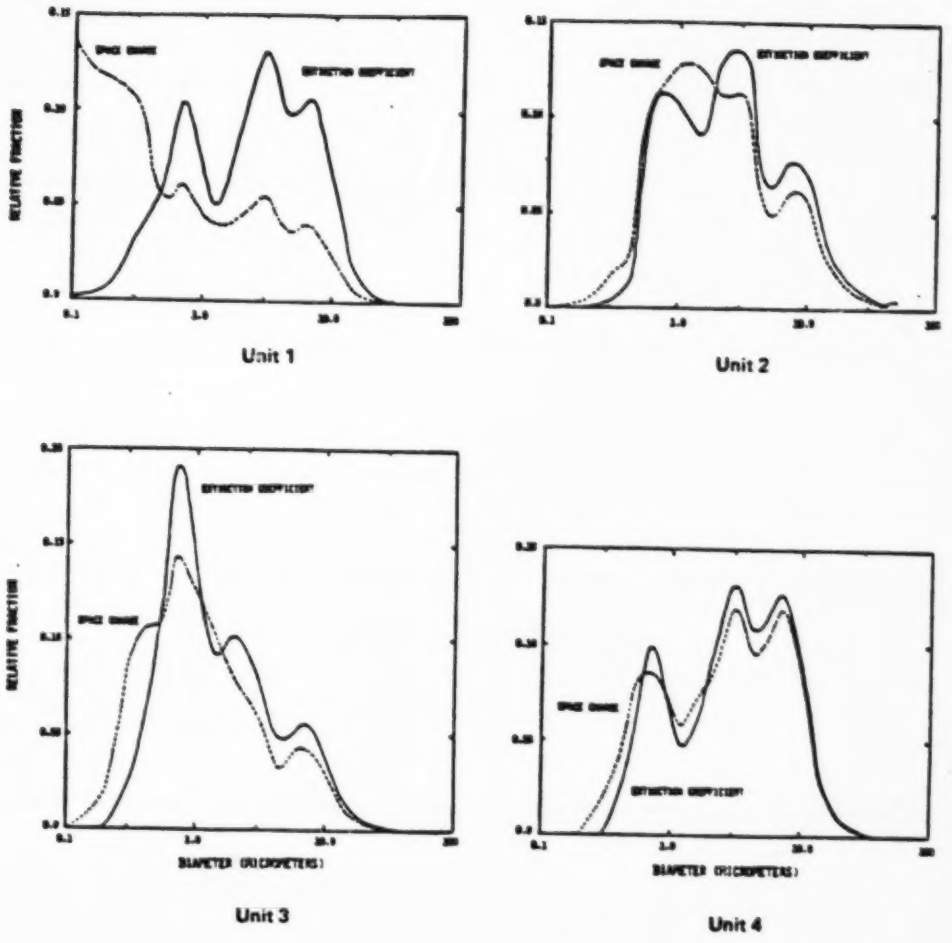

Figure 1. Space charge and extinction coefficient as functions of particle size for Unit 1 (industrial boiler), Unit 2 (utility hot-side), Unit 3 (utility cold-side), and Unit 4 (utility cold-side).

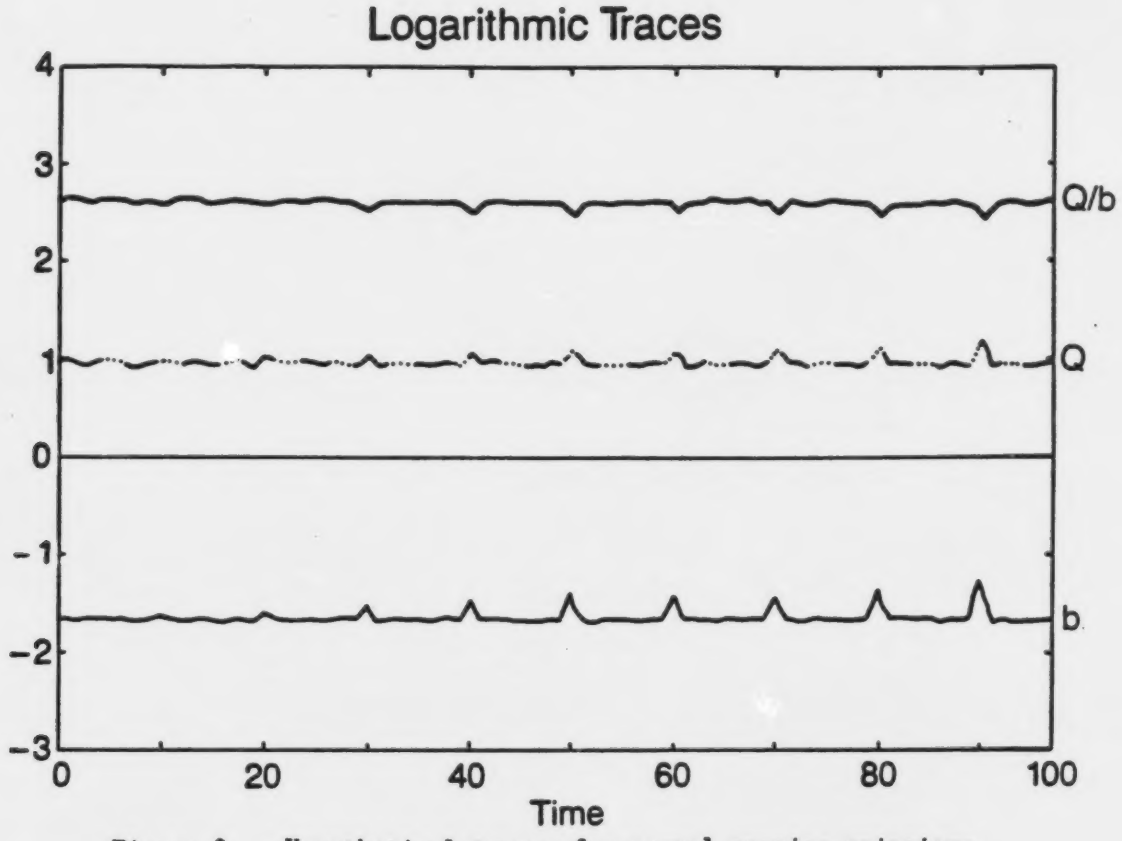

Figure 2. Hypothetical traces for normal rapping emissions.

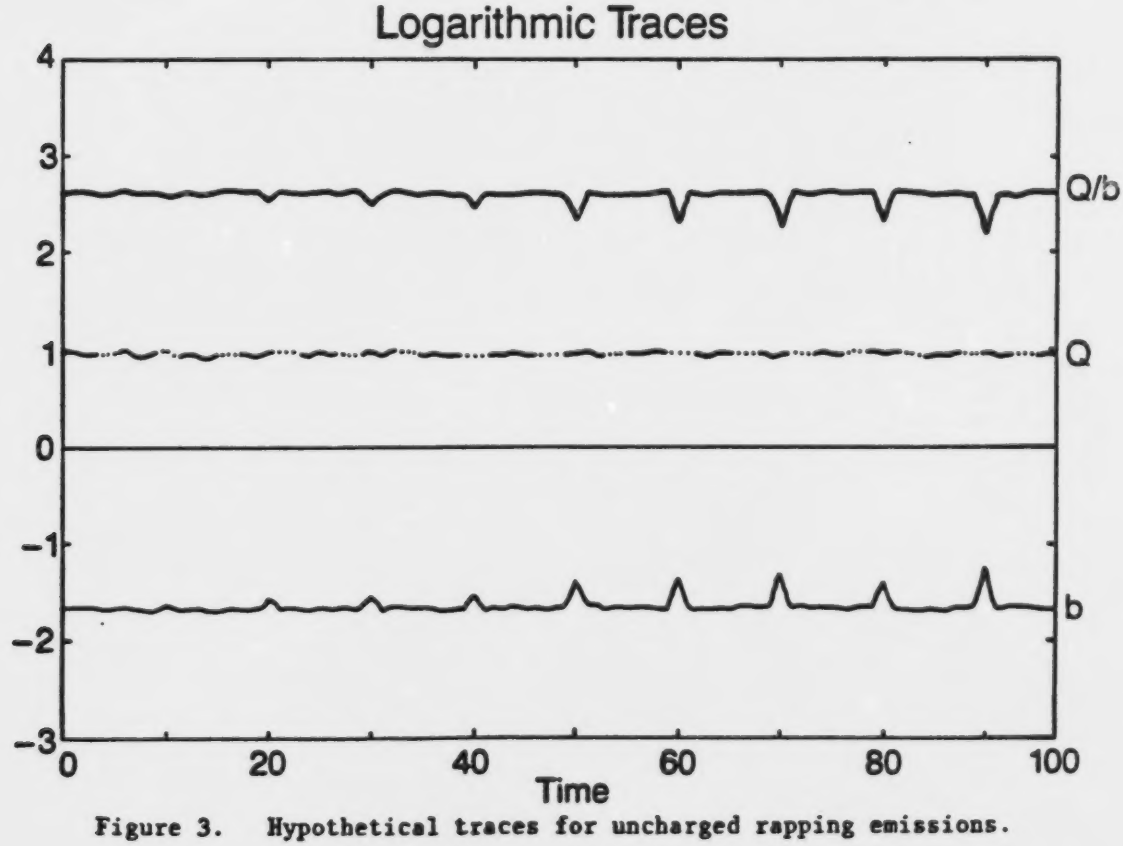

Figure 3. Hypothetical traces for uncharged rapping emissions.

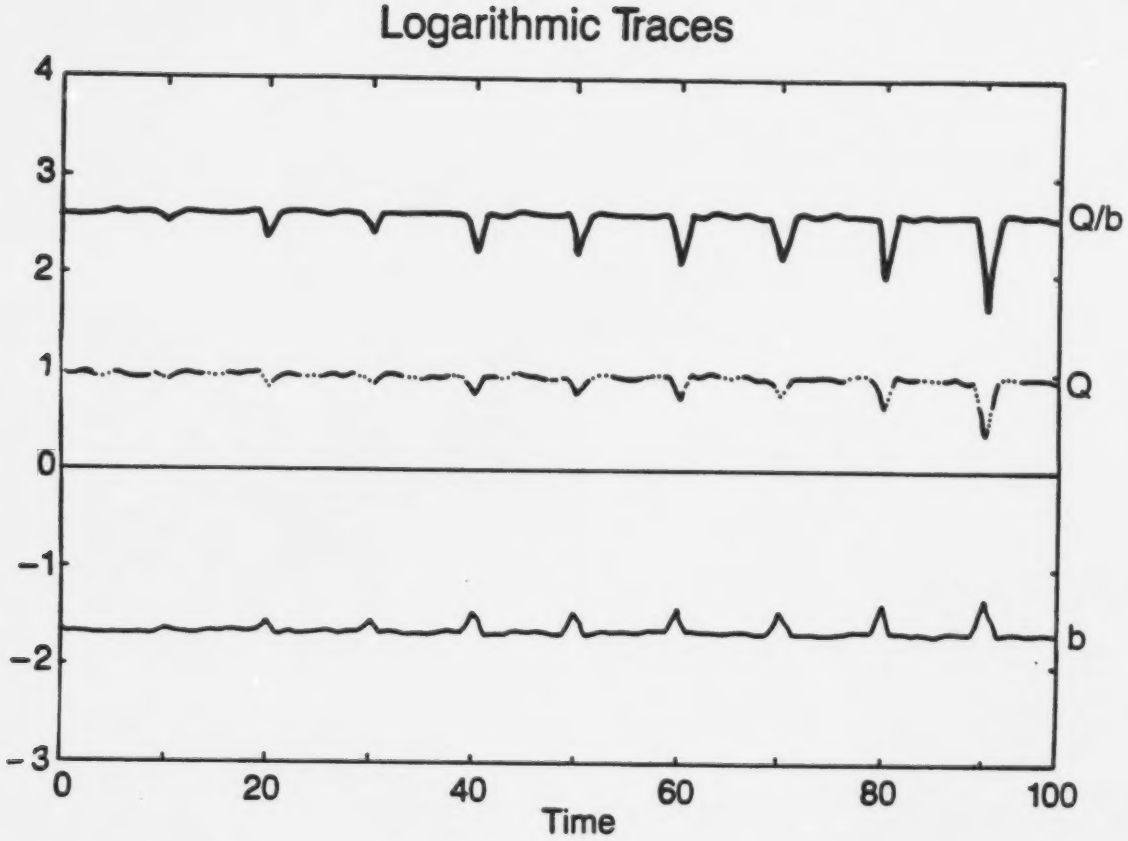

Figure 4. Hypothetical traces for opposite polarity rapping emissions.

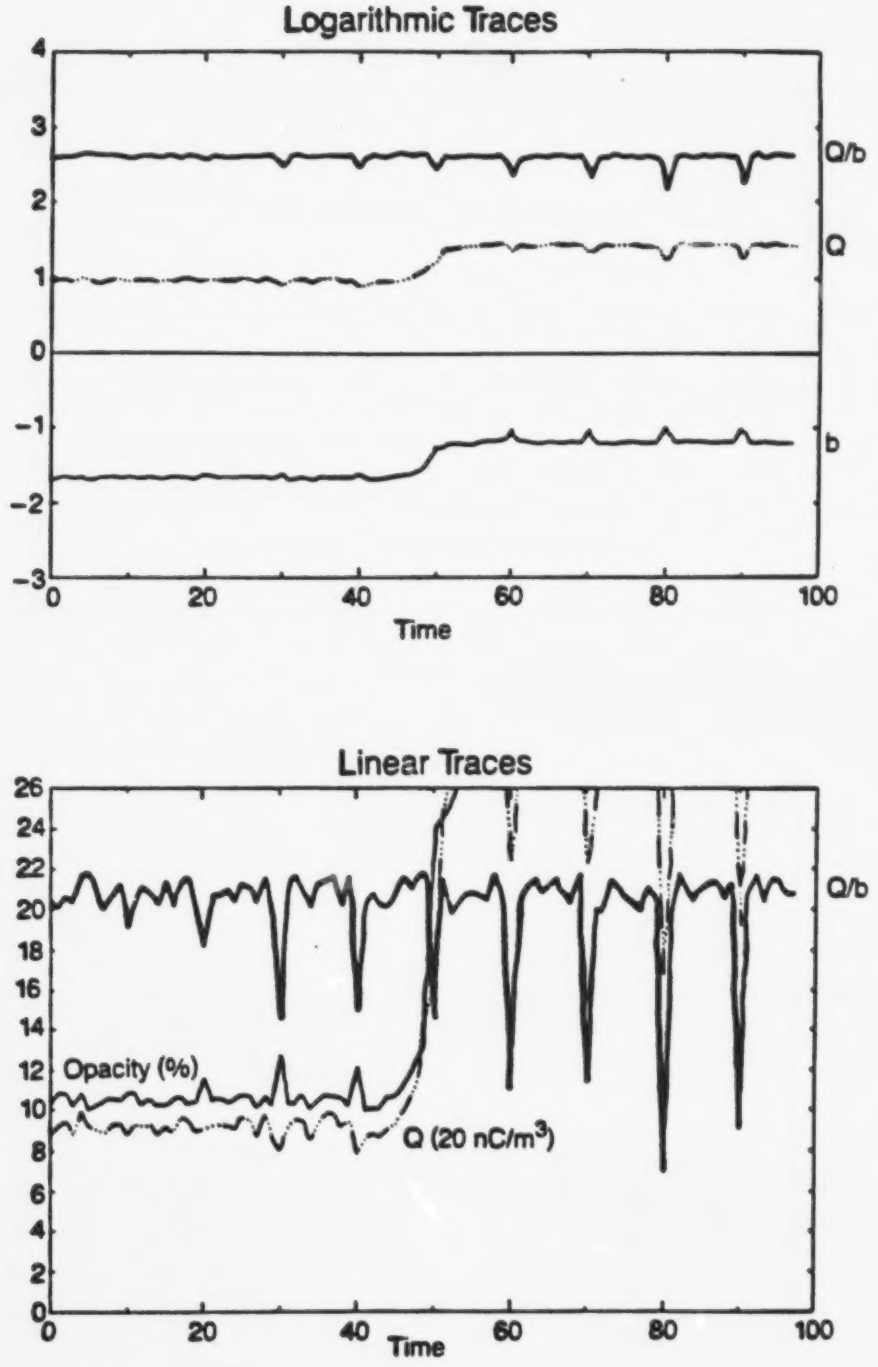

Figure 5. Hypothetical traces for an electrical section failure.

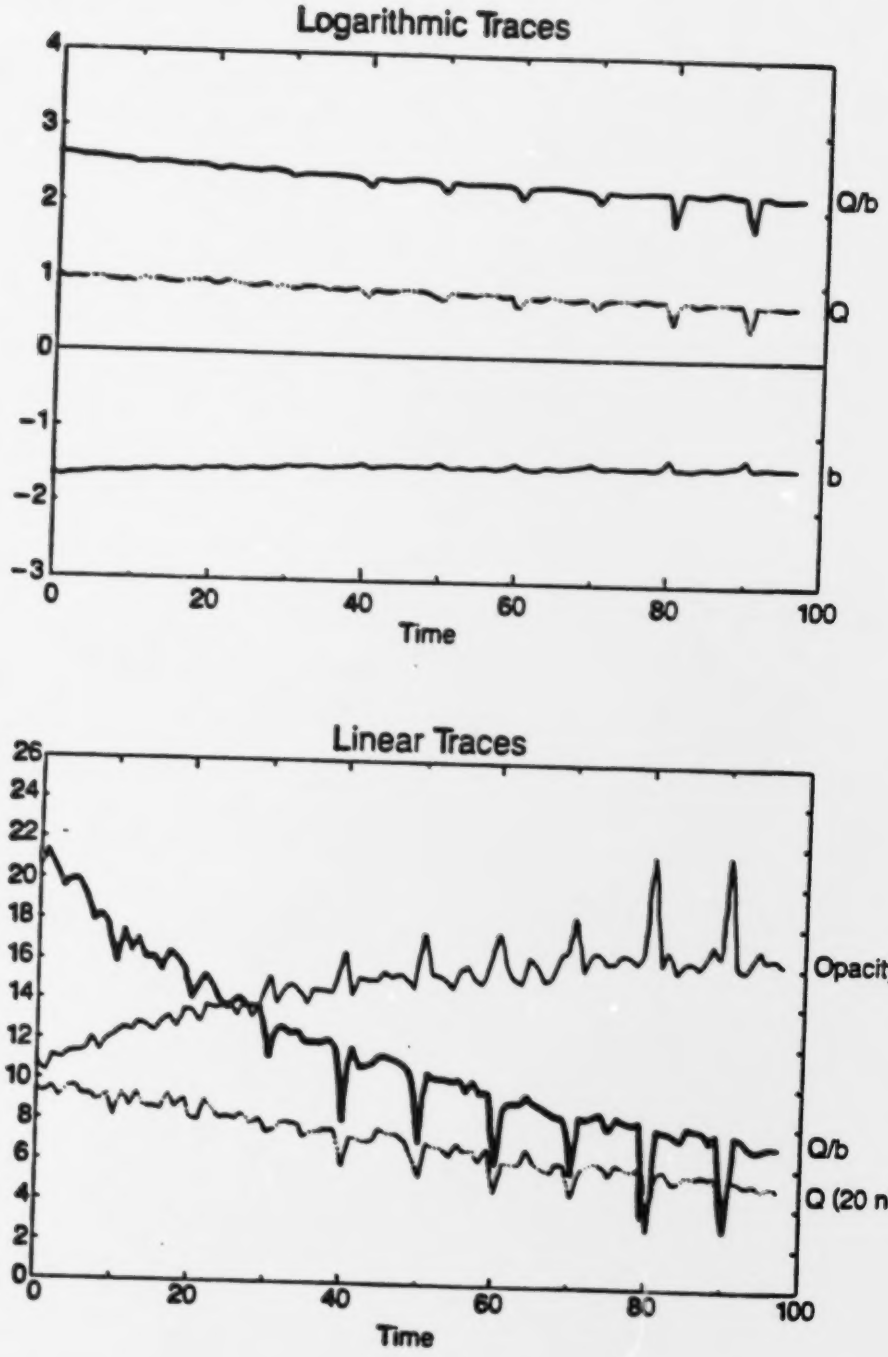

Figure 6. Hypothetical traces for the onset of back corona.